Table S1. Data collection and refinement statistics.

	HIV-2_{CTD}
Data Collection	
Wavelength (Å)	0.979
Resolution range (Å)	24.4 - 1.98 (2.05 - 1.98)
Space group	*C*2
Unit cell	
a,b,c (Å)	48.813, 30.919, 46.494
α,β,γ (°)	90, 90.561, 90
Total reflections	13142 (1335)
Unique reflections	4779 (489)
Multiplicity	2.7 (2.7)
Completeness (%)	95.44 (95.66)
I/σ(I)	11.41 (3.29)
R-merge	0.0624 (0.267)
R-meas	0.0762 (0.326)
R-pim	0.0430 (0.185)
$CC_{1/2}$	0.997 (0.963)
Refinement	
Reflections used	4761 (485)
# for R-free	237 (27)
R-work	0.2239 (0.3252)
R-free	0.2495 (0.3944)
Number of non-hydrogen atoms	659
Macromolecules	644
Solvent	15
Protein residues	83
RMSD	
Bond lengths (Å)	0.003
Bond angles (°)	0.60
Ramachandran plot	
Favored (%)	97.53
Allowed (%)	2.47
Outliers (%)	0.00
Average B-factor	49.45
Macromolecules	49.62
Solvent	42.34

Statistics for the highest-resolution shell are shown in parentheses.

Table S2. Cryo-EM data collection

Imaging Mode	Single Particle	Cryo ET
Data Collection		
Microscope	FEI Titan Krios	FEI Titan Krios
Voltage (kV)	300	300
Magnification	105,000×	105,000×
Energy-filter (eV)	20	20
Detector	Gatan K2 Summit	Gatan K2 Summit
Recording Mode	Super-resolution	Super-resolution
Pixel size (Å/pixel)	1.32	1.32
Defocus range setting (μm)	0.75 to 2.25	2.5
Total Dose ($e^-/Å^2$)	50-60	50
Dose rate (e^-/sec/pixel)	8.7	1.1
Exposure time (sec)	10.0	2.0
Frame number	40	8 per tilt
Dataset size	2508 micrographs	63 tilt series
Tilt range	N/A	±60
Tilt step	N/A	3

Table S3. HIV-2 lattice morphology

Index	Tomogram	N. of initial sampling points	Radius (nm)	Surface area coverage (%)	N. of Gag molecules
1	HIV2ts3_02	31067	66	88	5364
2	HIV2ts3_02	30220	64	78	4734
3	HIV2ts3_02	36533	71	78	5724
4	HIV2ts3_02	14930	45	63	2100
5	HIV2ts3_02	27651	62	70	3996
6	HIV2ts3_02	17142	62	N/A	2670
7	HIV2ts3_03	36909	71	76	5532
8	HIV2ts3_03	33605	68	75	5112
9	HIV2ts3_03	22931	56	72	3378
10	HIV2ts3_03	23501	57	83	3702
11	HIV2ts3_03	23053	56	66	3378
12	HIV2ts3_27	26151	60	79	4104
13	HIV2ts3_27	24491	58	74	3666
14	HIV2ts3_27	27088	61	83	4284
15	HIV2ts3_27	21712	55	89	3624
16	HIV2ts3_27	22541	56	76	3468
17	HIV2ts3_27	32274	69	N/A	4956
18	HIV2ts3_37	23008	56	78	3702
19	HIV2ts3_37	26910	61	80	4302
20	HIV2ts3_37	21962	55	75	3384
21	HIV2ts3_37	12483	42	61	1674
22	HIV2ts3_49	25778	60	88	4398
23	HIV2ts3_49	18761	51	59	2466

24	HIV2ts3_49	20685	61	N/A	3720
25	HIV2ts3_49	23272	57	81	3768

Note:

1) Particles #6, 17, and 24 are not full particles in the tomograms and were excluded from the calculation of the surface area coverage.
2) The radius of the Gag lattice is defined as the radius of the linker region (between $CA_{NT}D$ and CA_{CTD}) of the CA density layer.

Movie S1.

Model of a HIV-2 immature particle. The model is generated by placing the 5.5 Å CA hexamer density onto the Gag lattice determined by the StA Dynamo Gag hexamer position calculations. The NTD of the CA proteins are colored in blue and white. The CTDs and the CA-SP1 domains are colored in orange. The color denotes how well that hexamer matches the StA model, with blue having a higher correlation coefficient score than white.

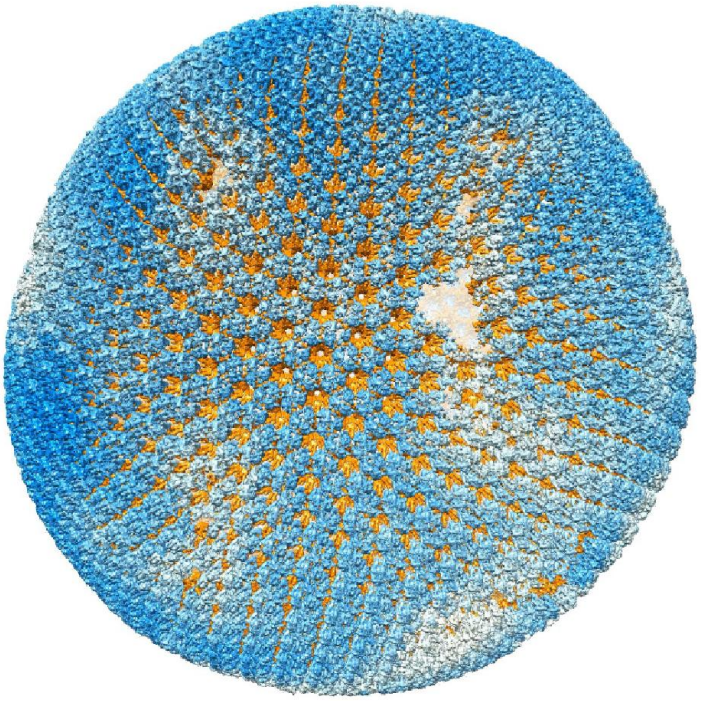

Figure S1

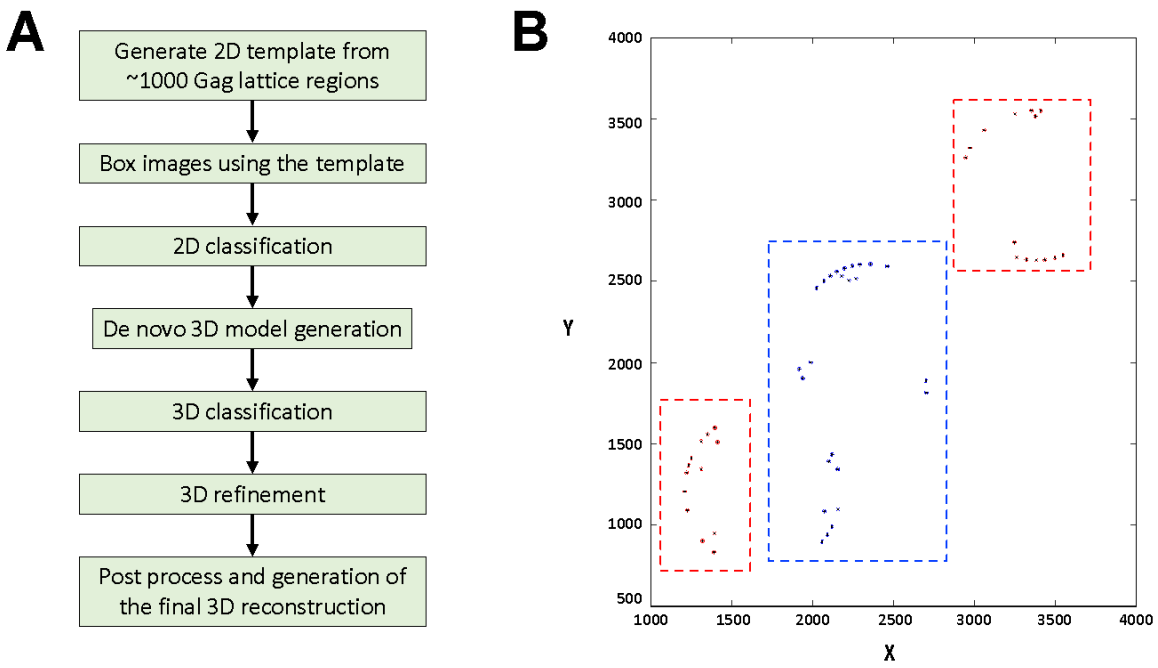

Figure S1. Workflow of cryo-EM single particle reconstruction. (A) The steps involved in calculating the 5.5 Å reconstruction map of HIV-2 Gag lattice structure. (B) Illustration showing the coordinates of the boxed particles sorted into two groups (blue and red) according to their locations in the micrograph. The two half sets are used for for resolution determination according to gold standard refinement procedures [70]

Figure S2

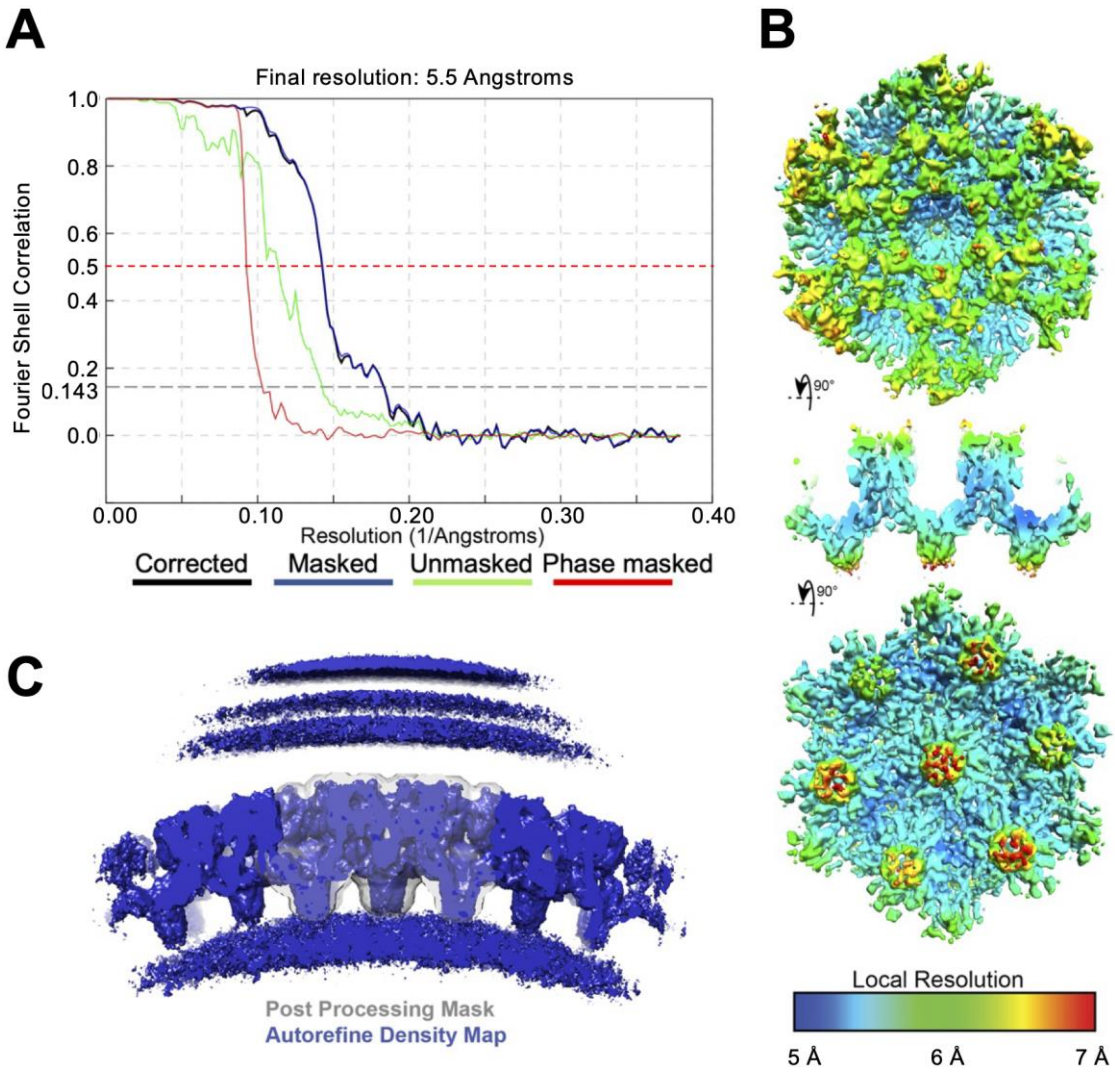

Figure S2. Cryo-EM structure validation of SPR of HIV-2 immature particles. (A) Gold standard FSC curves. (B) LocalRes result for the CA density in the reconstruction. (C) Central slice through the unmasked reconstruction density from 3D Autorefine along with CA mask used for generating the FSC curve in panel A.

Figure S3

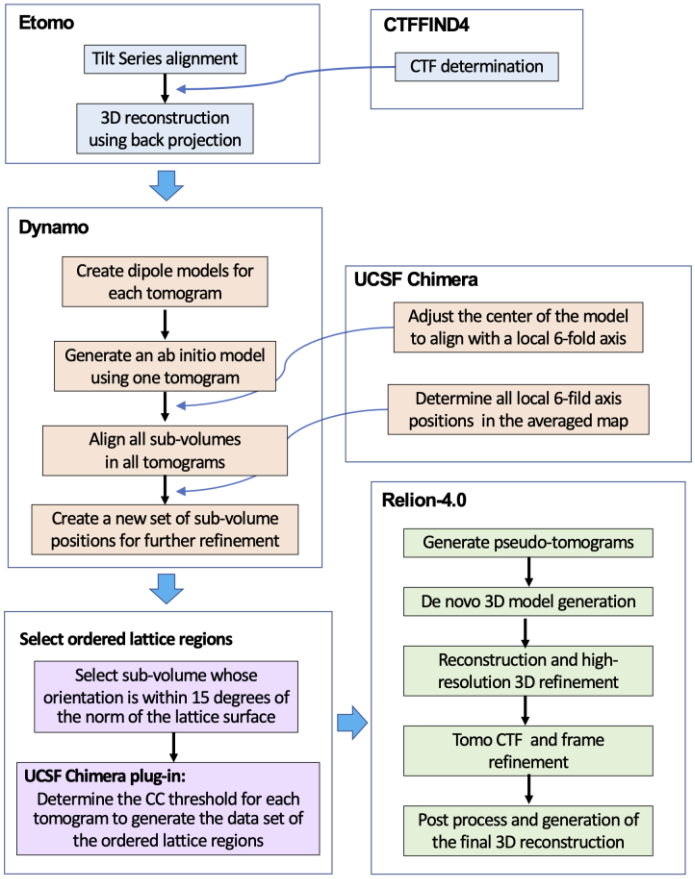

Figure S3. Workflow of cryo-ET and sub-tomogram averaging procedure. The software packages used in the cryo-ET and sub-tomogram averaging procedures include IMOD (Etomo) [65], CTFFIND4 [67], Dynamo [43], and RELION-4.0 [45]. The major computation steps for each software package are outlined in the respective box. The thick blue arrows represent the workflow of the sequential computational steps. The thin blue arrows represent information from CTFFIND4, and UCSF Chimera [69] is respectively integrated in the Etomo and Dynamo computations. The UCSF Chimera plug-in routine, Place Object [50], was used to determine the CC threshold for each tomogram to generate the data set of the ordered lattice regions.

Figure S4

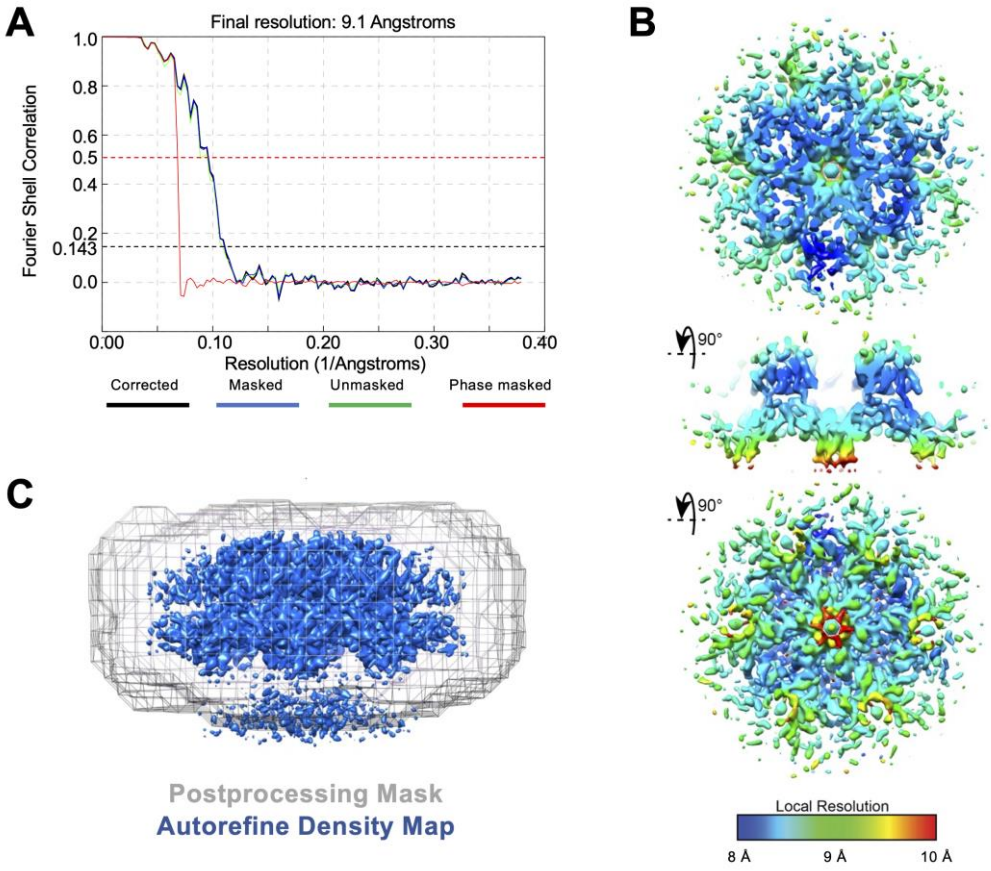

Figure S4. Resolution validation of HIV-2 immature particle Gag hexamer structure determined by the cryo-ET and sub-tomogram averaging methods. (A) Gold standard FSC curves. The resolution was determined to be 9.1 Å using FSC cut-off to be 0.143. (B) LocalRes result for the CA density in the reconstruction. (C) Sideview of the unmasked reconstruction density from 3D Autorefine along with the mask used for generating the FSC curve in panel A.

Figure S5

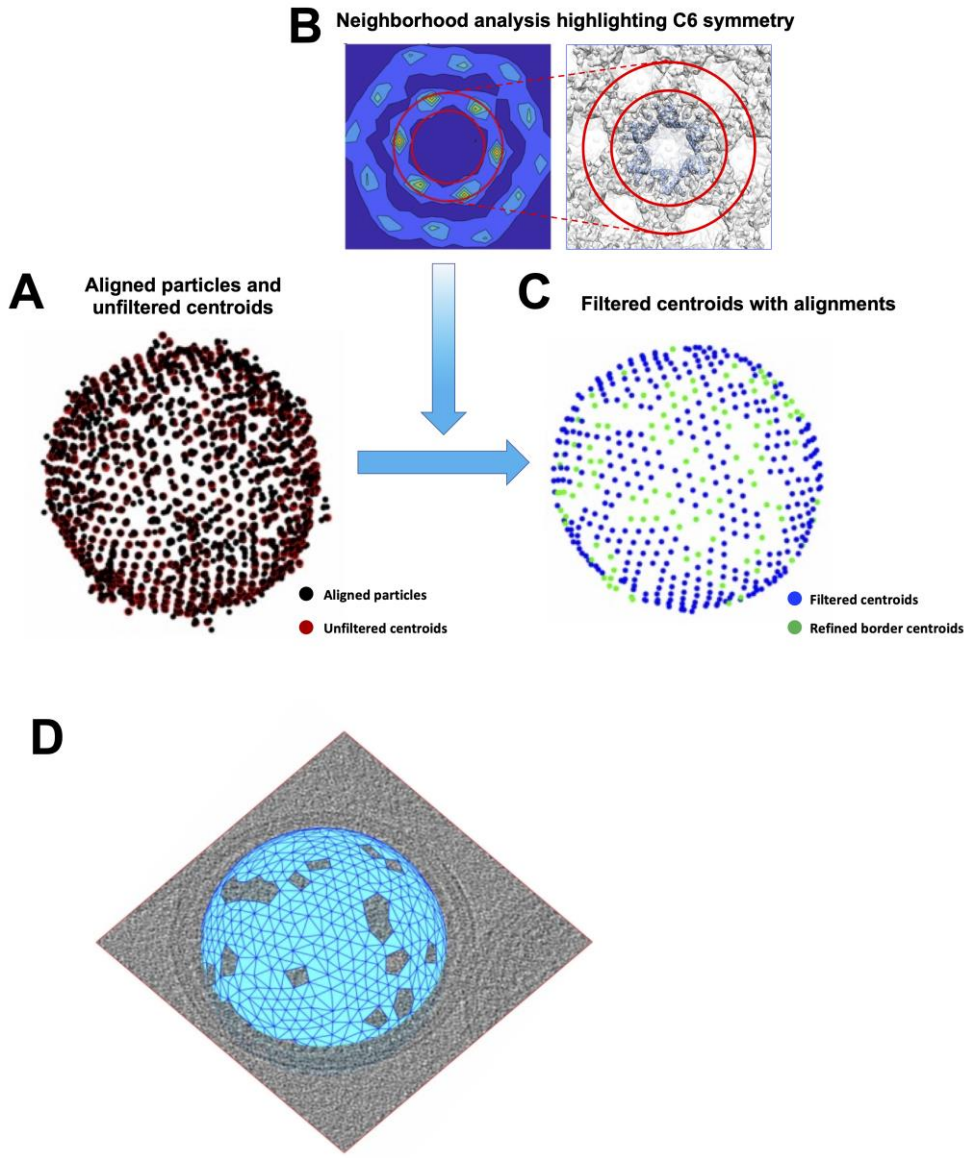
B
Neighborhood analysis highlighting C6 symmetry
A
Aligned particles and unfiltered centroids
C
Filtered centroids with alignments
Aligned particles
Unfiltered centroids
Filtered centroids
Refined border centroids
D

Figure S5. Scheme of the estimation procedure for the Gag layer coverage. (A) Estimated Gag hexamer positions based on the DBSCAN algorithm. A fine initial subtomogram sampling on the expected location of the Gag layer was used in an alignment project with the density map of a single Gag hexamer as a reference, leading to the aligned positions marked as black points. Using the DBSCAN algorithm to identify clusters of putative positions, the initial, unfiltered estimation of Gag hexamer centroids, marked as red points in the panel, are obtained. (B) The neighborhood analysis of unfiltered centroids is a region used for the neighborhood analysis of the initial estimations. The inherent C6 symmetry of the found neighboring Gag hexamer centroids is highlighted. The inner and outer red rings indicate distances of 6.6 and 7.9 nm radii respectively, corresponding to the apparent range of distances between two adjacent Gag hexamer centers. This emergence of the C6 symmetry of the Gag layer is used to filter the initial estimation of the Gag hexamer center positions. (C) Illustration of the Gag hexamer positions determined by the neighborhood analysis algorithm. As a result of this filtering, a subset of the unfiltered centroids was obtained, depicted as blue points, with a local lattice structure around them. This subset was increased by recovering the centroids in positions that follow the C6 symmetry with the filtered centroids. This allowed for refinement of the area on the borders of holes in the Gag lattice. (D) The final depiction of the Gag lattice layer on a HIV-2 immature particle. The blue mesh surface was used to calculate the percentage of the surface area that is covered by Gag hexamers.

Figure S6

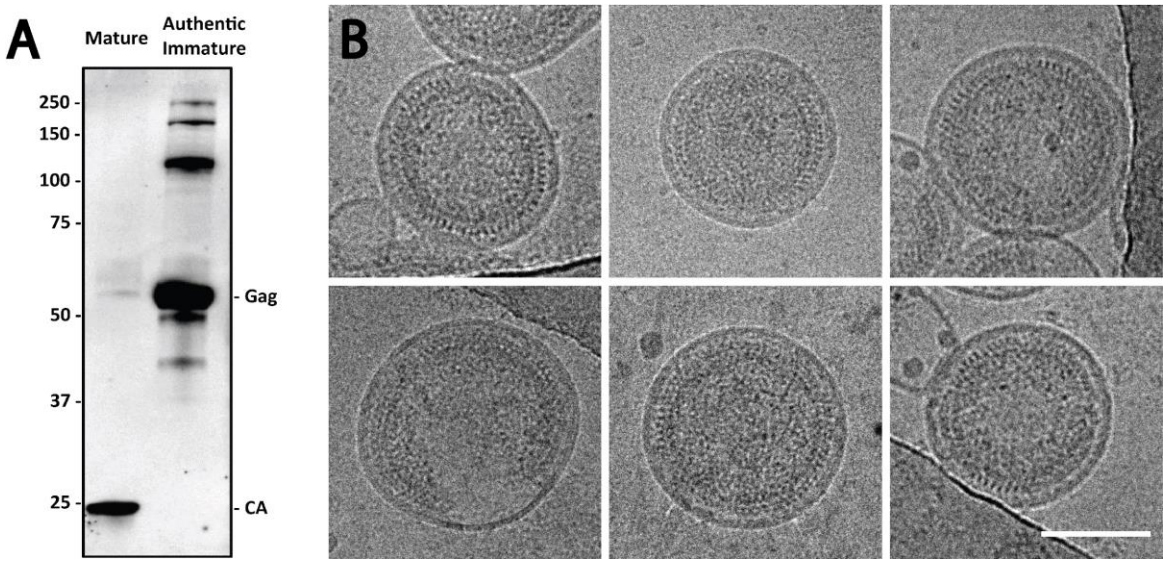

Figure S6. Immunoblot and cryo-EM analysis of authentic immature HIV-2 particles. (A) Immunoblot analysis of mature (WT) and authentic immature (protease catalytic domain mutant) HIV-2 particles using an anti-HIV-2 CA primary antibody which recognizes an epitope within the Gag CA region. (B) Cryo-EM images of authentic immature HIV-2 particles. The scale bar represents 100 nm.

Figure S7

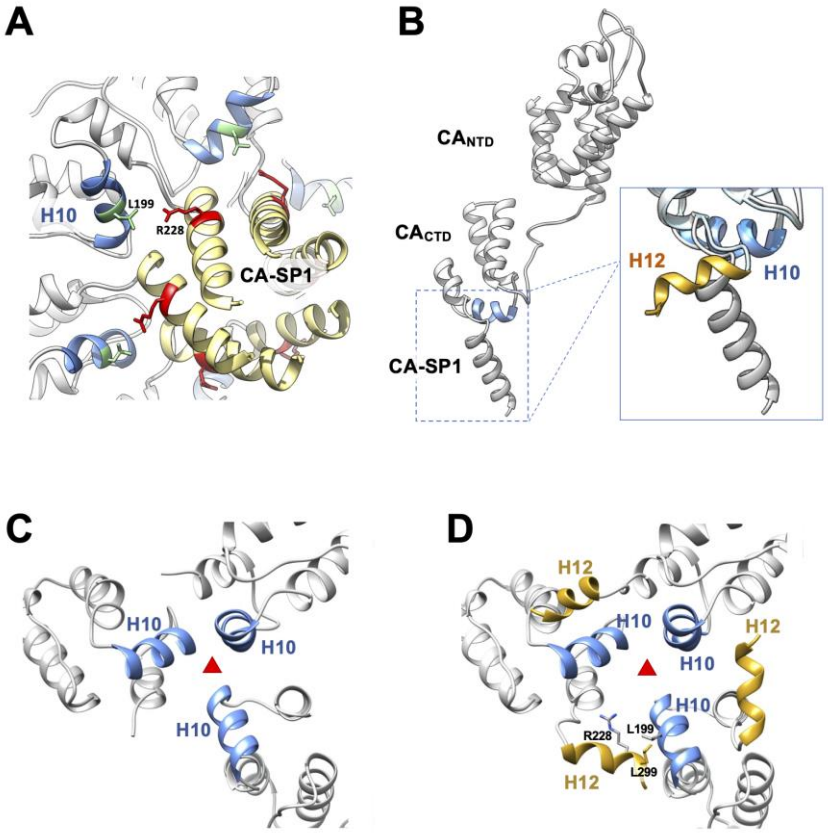

Figure S7. Modeling implications of HIV-2 CA H12 in the immature and mature lattice configuration. (A) Modeled HIV-2 CA and SP1 in the immature Gag lattice, showing CA-SP1 6HB (tan) and H10 (light blue). The residues L199 are colored in light green. The residues of R228 are colored red. (B) Superposition of HIV-2 CA_{CTD} crystal structure on to the HIV-2 immature CA and SP1 model (grey). H10 is colored in light blue, and H12 is colored in gold. Structural comparison shows that H12 of the crystal structure adopts a different conformation of the CA-SP1 helix of the immature CA model. (C) Three-fold interface of mature HIV-1 CA lattice (PDB ID: 6SKN) [71] with H10 indicated in light blue. (D) Three copies of HIV-2 CA_{CTD} fit to HIV-1 CA_{CTD} positions, revealing putative H10-12 interfaces. The red triangle represents the three-fold symmetry axis.

Figure S8

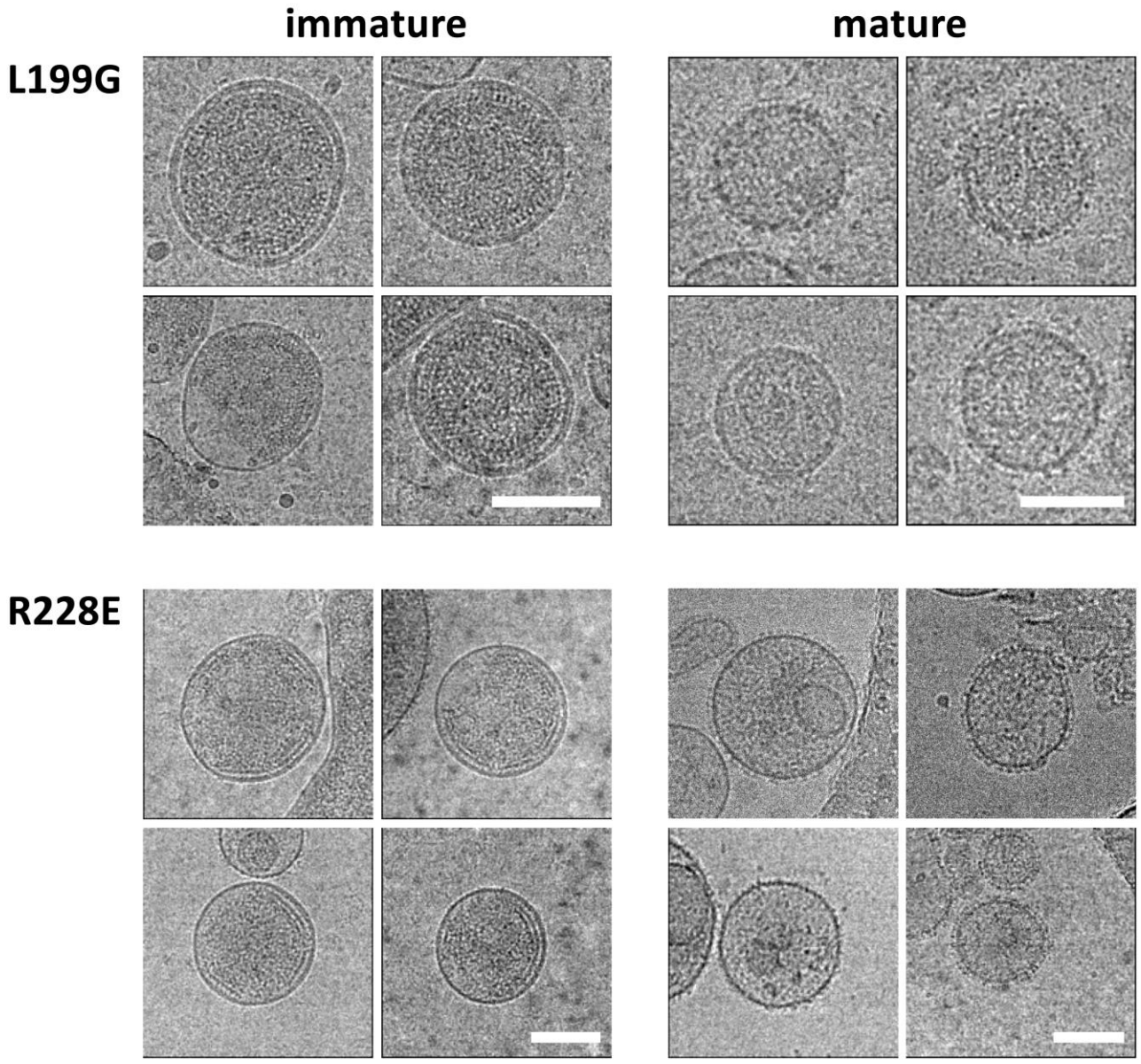

Figure S8. Morphology of HIV-2 Gag L199G and R228E immature and mature particles.

Cryo-EM images of the HIV-2 Gag L199G and R228E mutants reveal immature particles with ordered Gag assemblies (left) and the defective CA mature particles with the same mutations in Gag (right). The scale bars represent 100 nm.

Figure S9

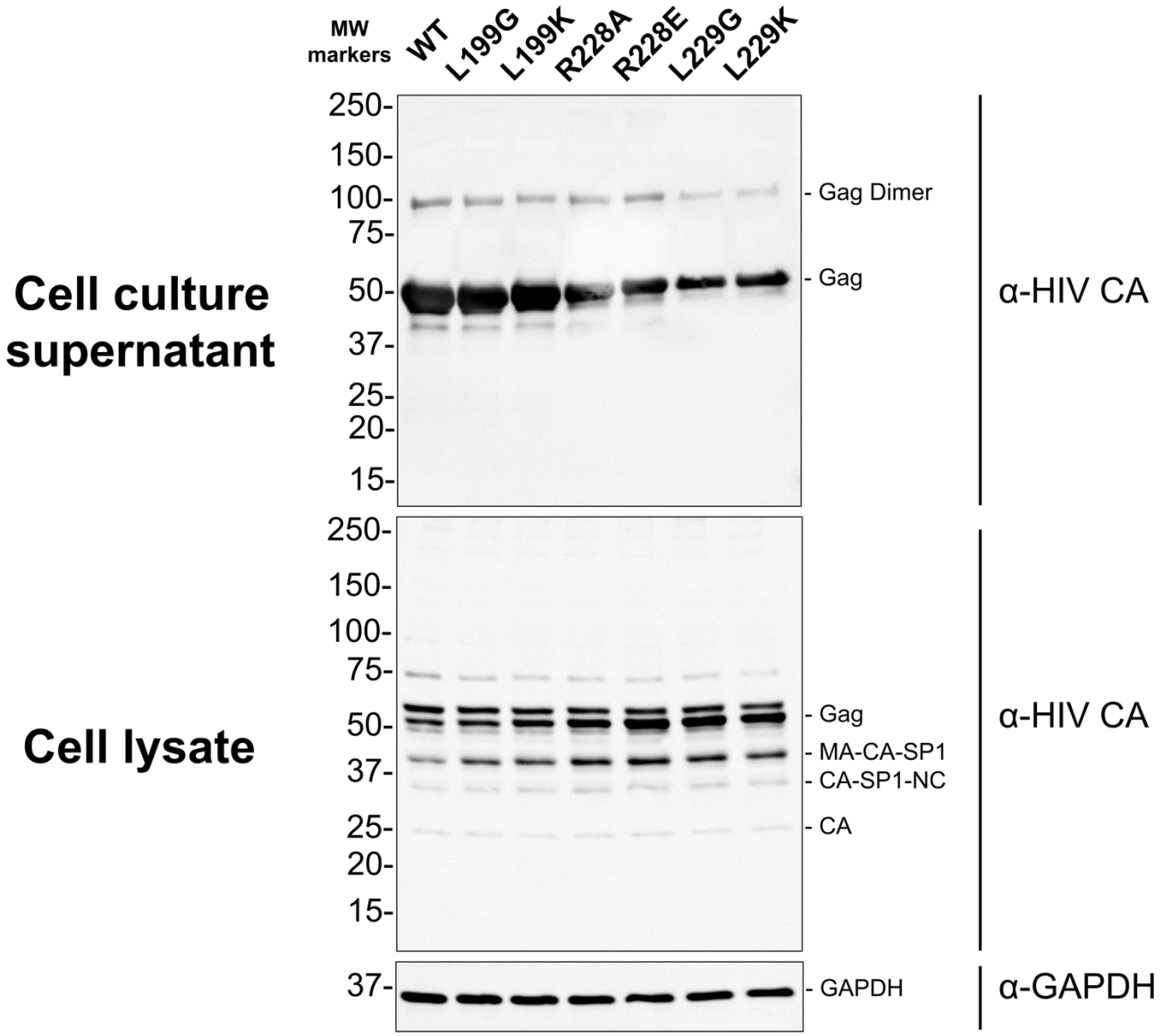
MW markers
WT
L199G
L199K
R228A
R228E
L229G
L229K
250-
150-
100-
75-
50-
37-
25-
20-
15-
- Gag Dimer
- Gag
α-HIV CA
Cell culture supernatant
250-
150-
100-
75-
50-
37-
25-
20-
15-
- Gag
- MA-CA-SP1
- CA-SP1-NC
- CA
α-HIV CA
Cell lysate
37-
- GAPDH
α-GAPDH

Figure S9. Immunoblot analysis of immature particle production for HIV-2 CA mutants. Immature particle production for HIV-2 CA mutants were analyzed by using an antibody directed against the CA domain of Gag. The Gag proteins from cell culture supernatants were detected with a 1:1500 dilution of anti-HIV-1 p24 antibody in 5% milk TBST and cell lysates were detected with 1:2000 dilution of anti-HIV-1 p24 antibody in 5% milk TBST. Glyceraldehyde 3-phosphate dehydrogenase (GAPDH) in cell lysate was detected by using a 1:10,000 anti-GAPDH antibody in 5% milk TBST. Membranes were washed before incubation with 1:5000 IRDye® 800CW goat anti-mouse IgG secondary antibody and 1:5000 IRDye® 680RD goat anti-rabbit IgG secondary antibody. Immunoblots were imaged by using a ChemiDoc Touch system and analyzed with ImageJ. Gag proteins and Gag cleavage products (i.e., Gag dimer, Gag, MA-CA-SP1, CA-SP1-NC, and CA) and GAPDH (to ensure equal loading of cell lysates) are identified. The sizes of the molecular weight (MW) markers are indicated along the left side of the immunoblot.

Figure S10

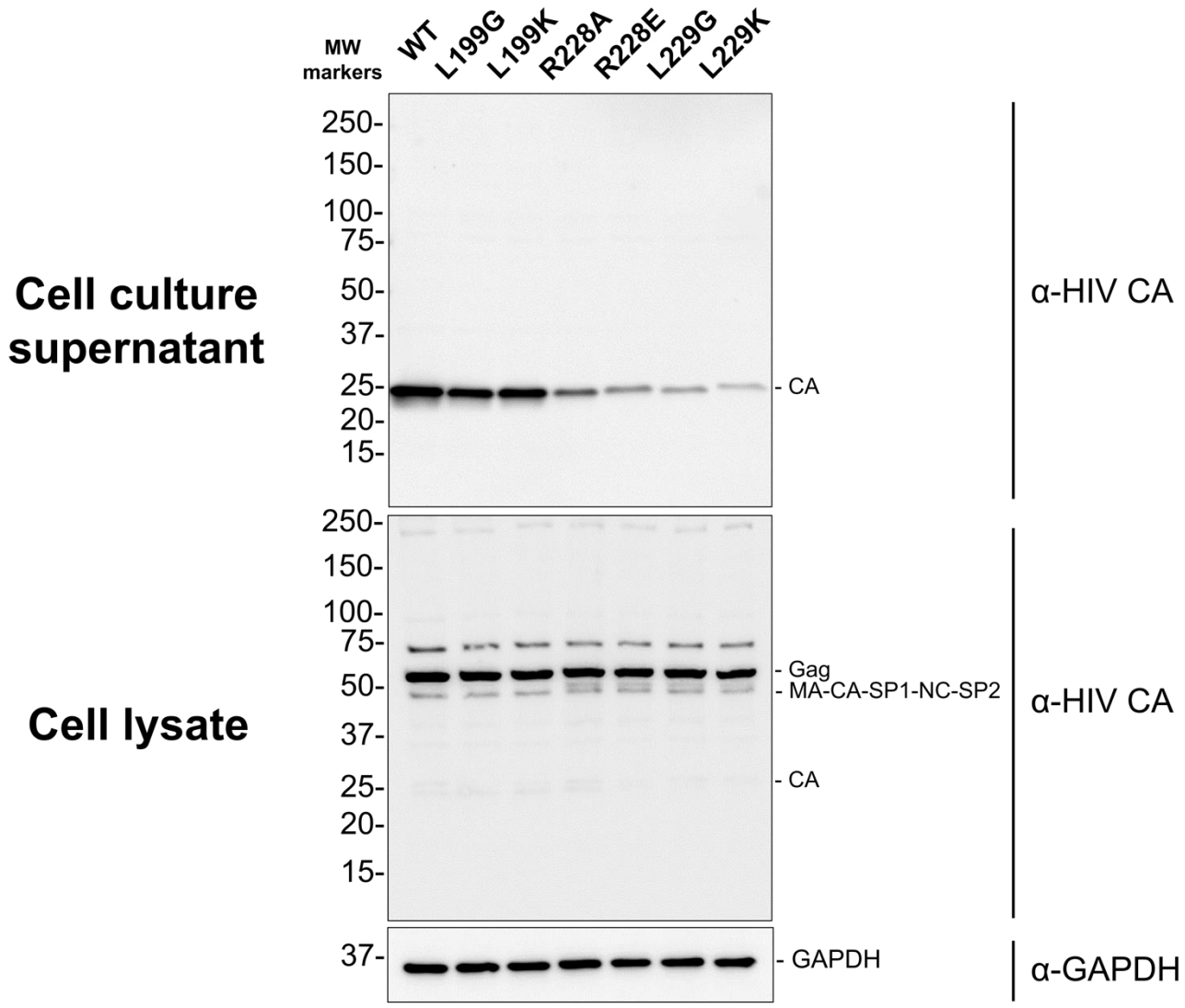
MW markers
WT
L199G
L199K
R228A
R228E
L229G
L229K
250-
150-
100-
75-
50-
37-
25-
20-
15-
Cell culture supernatant
- CA
α-HIV CA
Cell lysate
- Gag
- MA-CA-SP1-NC-SP2
- CA
α-HIV CA
37-
- GAPDH
α-GAPDH

Figure S10. Immunoblot analysis of mature particle production for HIV-2 CA mutants. Mature particle production for HIV-2 CA mutants were analyzed by using an antibody directed against the CA domain. The CA proteins from cell culture supernatants were detected with a 1:1500 dilution of anti-HIV-1 p24 antibody in 5% milk TBST (**Figure 5B**) and cell lysates were detected with 1:2000 dilution of anti-HIV-1 p24 antibody in 5% milk TBST. Glyceraldehyde 3-phosphate dehydrogenase (GAPDH) in cell lysate was detected by using a 1:10,000 anti-GAPDH antibody in 5% milk TBST. Membranes were washed before incubation with a 1:5000 IRDye® 800CW goat anti-mouse IgG secondary antibody and 1:5000 IRDye® 680RD goat anti-rabbit IgG secondary antibody. Immunoblots were imaged by using a ChemiDoc Touch system and analyzed with ImageJ. Gag proteins and Gag cleavage products (i.e., Gag-Pol, Gag, MA-CA-SP1-NC-SP2, and CA) and GAPDH (to ensure equal loading of cell lysates) are identified. The sizes of the molecular weight (MW) markers are indicated along the left side of the immunoblot.

Figure S11

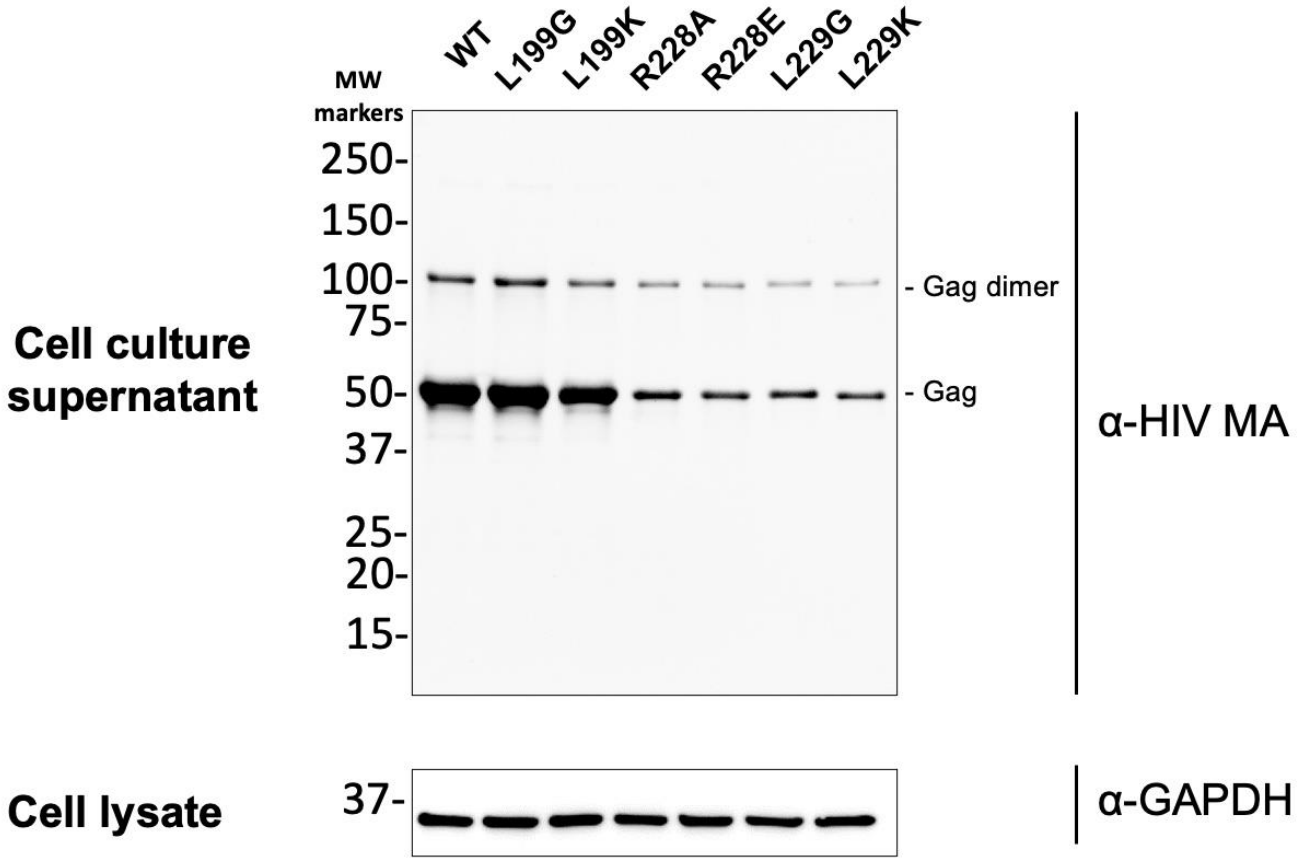
WT
L199G
L199K
R228A
R228E
L229G
L229K
MW markers
250-
150-
100-
75-
50-
37-
25-
20-
15-
- Gag dimer
- Gag
Cell culture supernatant
α-HIV MA
37-
Cell lysate
α-GAPDH

Figure S11. Confirmation of immature particle production for HIV-2 CA mutants by using anti-MA antibody. Immature particle production for HIV-2 CA mutants were analyzed by using an antibody directed against the MA domain of Gag (rather than an anti-CA antibody). Gag protein from culture supernatants were detected with a 1:1000 dilution of anti-HIV-1 p17 antibody in 5% milk TBST. Membranes were washed before incubation with a 1:6000 IRDye® 800CW goat anti-mouse IgG secondary antibody. Immunoblots were imaged by using a ChemiDoc Touch system and analyzed with ImageJ. Shown is a representative immunoblot from cell culture supernatant and the GAPDH from cell lysates to confirm particle production from comparable numbers of cells.